Barometric Height Estimation Combined with Map-Matching in a Loosely-Coupled Kalman-Filter

Maik Bevermeier, Oliver Walter, Sven Peschke and Reinhold Haeb-Umbach
Department of Communications Engineering
University of Paderborn, Germany
{bevermeier, walter, peschke, haeb}@nt.uni-paderborn.de

***Abstract*—In this paper we present a robust location estimation algorithm especially focused on the accuracy in vertical position. A loosely-coupled error state space Kalman filter, which fuses sensor data of an Inertial Measurement Unit and the output of a Global Positioning System device, is augmented by height information from an altitude measurement unit. This unit consists of a barometric altimeter whose output is fused with topographic map information by a Kalman filter to provide robust information about the current vertical user position. These data replace the less reliable vertical position information provided the GPS device. It is shown that typical barometric errors like thermal divergences and fluctuations in the pressure due to changing weather conditions can be compensated by the topographic map information and the barometric error Kalman filter. The resulting height information is shown not only to be more reliable than height information provided by GPS. It also turns out that it leads to better attitude and thus better overall localization estimation accuracy due to the coupling of spatial orientations via the Direct Cosine Matrix. Results are presented both for artificially generated and field test data, where the user is moving by car.**

***Index Terms*—Loosely-coupled error state space Kalman filter, Inertial Measurement Unit, Barometric heigth estimation, Error filtering, Map-Matching.**

I. Introduction

In the last years, vehicle positioning has become more and more important, as many emerging applications rely on accurate vehicle location information, such as Car-2-Car communication or traffic and fleet management systems, to name just a few.

Most vehicle positioning approaches are based on a combination of sophisticated sensors and external data sources. Often a GPS device is used to sustain data of an Inertial Measurement Unit (IMU) by the strapdown calculation [1], [3], [5]. The accuracy of the position estimates depends on the quality of the GPS pseudorange (range from satellite to user measured by envelope delay) and optional deltarange measurements (relative velocity measurement due to Doppler effect) as well. A well known disadvantage of GPS systems is that they provide less accurate information about the vertical position. The standard deviation of the error of the estimated height is often more than $10\,\mathrm{m}$ [4]. This is a deficit considering a situation, where a car is to be tracked, which is located on a bridge when crossing another street. Another example which asks for accurate height information is a traffic management system which has to guide the driver to a free parking lot in a multi-level parking garage. In areas, where the visibility of satellites is limited by high buildings, even complete dropouts of the GPS signal can occur [6]. Another challenging but nevertheless important area is indoor navigation, where a GPS signal is often unavailable. In this case, the computation of the attitude depends on the IMU, which quickly leads to unreliable track estimates. In all these situations additional sensor devices are required to support the localization. A barometer could be one such device, as it is cheap and often delivers more precise vertical position information than GPS.

In this paper we consider a loosely-coupled error state space Kalman filter, where IMU sensor information (gyroscope, magnetometer and accelerometer), GPS satellite based position information and barometric altitude information are jointly used. Before fusion in the error state space Kalman filter, the errors of the barometer data, which e.g. result from weather conditions (changes in temperature and pressure) are reduced by a second Kalman filter, which is supported by topographic map data. This means, that if the estimated horizontal position corresponds to a location, for which height information is available from the topographic map, both the height reading of the map and the barometer output are used for the current error filtering step. To find this out we compare the current user position with the horizontal positions in a database, storing the topographic information. This is necessary since a topographic map provides height information only for certain horizontal positions. However, the information obtained from topographic maps are often more accurate than comparable information of street maps used in combination with GPS based positioning. In most low cost navigation applications map information is not used. The vertical position is obtained from the GPS device directly.

This paper is organized as follows. In the next section we explain our artificial data generation system comprising error modeling for the IMU and the GPS. Further, we provide some details about the field measurements also used in this paper. The loosely-coupled error state space Kalman filter for the correction of the IMU data is described in detail in section III. The Kalman filtering with map-matching for the height estimation is explained in section IV. There we will go into details about barometric height estimation and explain how the errors depend on weather conditions. We present results concerning the performance of the algorithm compared to a non-barometric aided loosely-coupled filter in section V. Further, we consider the performance during GPS dropouts.

Results are given for the artificially generated data and real-world measurements recorded in field tests. The paper finishes with conclusions drawn in section VI.

II. Data Generation

As a sufficient amount of field data was not available we also generated artificial sensor data of a GPS and IMU device to assess the performance of the proposed approach for sensor fusion.

A. Artificial Data Generation

We assume that the IMU consists of a magnetometer, an accelerometer and a gyroscope for measuring angular velocities. These devices can be found in most vehicles, e.g. to be used for the electronic stability program (ESP).

1) Ideal Trajectory and IMU Measurements: For the generation of trajectories we used an interaction between three different linear moving models: 'constant velocity', 'constant acceleration' and 'turning' motion (fig. 1) [6]. Note, that all vectors in the chart are time-dependent, which we did however not indicate in the notation for simplicity reasons. The system

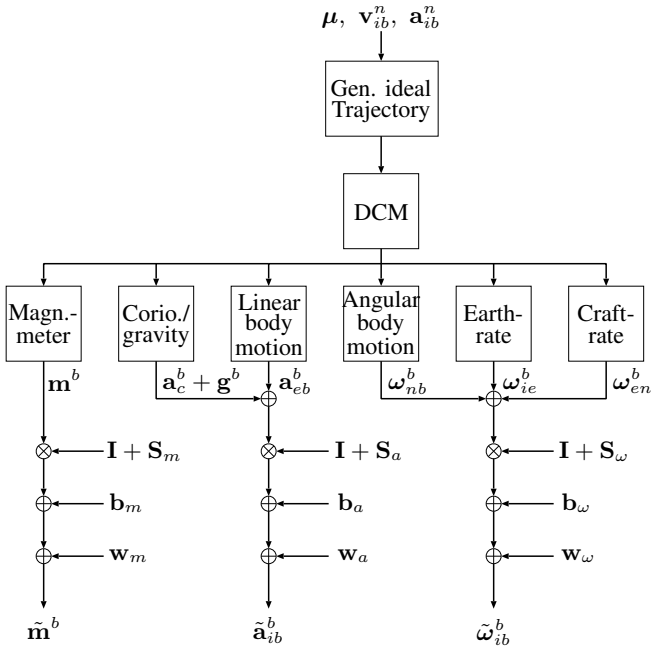

Fig. 1. Data generation chart for the IMU (DCM: Direct Cosine Matrix).

expects at its input the Euler angle vector $\boldsymbol{\mu} = [\phi, \theta, \psi]^T$ as well as the velocity and acceleration vectors $\mathbf{v}_{ib}^n$ and $\mathbf{a}_{ib}^n$. The indices denote the velocity or acceleration vector of the body motion in body frame b with respect to the inertial navigation frame i given in coordinates of the n-frame (also known as NED-frame) with the coordinate axes north, east and down. After the generation of the ideal trajectory the required Direct Cosine Matrices (DCMs) transforming data from one coordinate system into another are computed for further use. The earth rotation and the craft-rate $\boldsymbol{\omega}_{en}^b$ in body coordinates is incoporated in the data generation as well as the coriolis force $\mathbf{a}_c^b$ and gravity vector $\mathbf{g}^b$. All vectors, the ideal magnetometer data $\mathbf{m}^b$, the angular velocities $\boldsymbol{\omega}_{ib}^b$ and the linear accelerations $\mathbf{a}_{ib}^b$ are then distorted by scaling errors $\mathbf{S}_a$, $\mathbf{S}_\omega$ and $\mathbf{S}_m$, biases $\mathbf{b}_a$, $\mathbf{b}_\omega$ and $\mathbf{b}_m$ and noise terms $\mathbf{w}_a$, $\mathbf{w}_\omega$ and $\mathbf{w}_m$ to obtain the simulated sensor data $\tilde{\mathbf{m}}^b$, $\tilde{\mathbf{a}}_{ib}^b$ and $\tilde{\boldsymbol{\omega}}_{ib}^b$. The biases of angular velocity and linear acceleration are modeled by random walk processes according to

$$\mathbf{b}_a(k) = \mathbf{b}_a(k-1) + \boldsymbol{\eta}_a(k) \cdot \sqrt{\Delta t} \tag{1}$$

$$\mathbf{b}_\omega(k) = \mathbf{b}_\omega(k-1) + \boldsymbol{\eta}_\omega(k) \cdot \sqrt{\Delta t}, \tag{2}$$

while $\mathbf{b}_m$ is set to zero ($\mathbf{b}_m = \mathbf{0}$), which means that we neglect the bias of the magnetometer in the following. Δt denotes the IMU sampling time.

The vectors $\boldsymbol{\eta}_a$ and $\boldsymbol{\eta}_\omega$ are zero mean Gaussians with (3×3) covariance matrices $\boldsymbol{\sigma}_{b_a}^2$ and $\boldsymbol{\sigma}_{b_\omega}^2$. The inherent noise terms $\mathbf{w}_\omega$, $\mathbf{w}_a$ and $\mathbf{w}_m$ are assumed to be each zero mean with variances $\boldsymbol{\sigma}_\omega^2$, $\boldsymbol{\sigma}_a^2$, and $\boldsymbol{\sigma}_m^2$, respectively: $\mathbf{w}_\omega(k) \sim \mathcal{N}(\mathbf{0}, \boldsymbol{\sigma}_\omega^2), \mathbf{w}_a(k) \sim \mathcal{N}(\mathbf{0}, \boldsymbol{\sigma}_a^2), \mathbf{w}_m(k) \sim \mathcal{N}(\mathbf{0}, \boldsymbol{\sigma}_m^2)$. The scaling factor matrices $\mathbf{S}_a$, $\mathbf{S}_\omega$ and $\mathbf{S}_h$ are assumed to be diagonal, i.e. we assume that there is no misalignment between the individual sensor axes. Further, the matrices are assumed to be known at receiver side.

2) GPS Measurements: The GPS reference data generation and measurement simulation block contains a Kalman filter as is used in a typical GPS receiver. First, we generate typical satellite positions by using ideal Kepler parameters with respect to the current user location. Then we produce pseudorange and deltarange measurements incorporating, among others, ionospheric, tropospheric and thermal effects. Also multipath errors are incorporated. These measurements are merged in the vector $\mathbf{z}_{p,d}$, which is input to the GPS Kalman filter, which estimates the user longitude λ and latitude φ, the corresponding velocities and the receiver clock drift, which can be used as measurements for the successive filter algorithms. Here, we only use the position and velocity estimates merged in vector $\hat{\mathbf{x}}_{\text{GPS}}$, as well as the estimation error covariance matrix $\hat{\mathbf{P}}_{\text{GPS}}$ as described in the following sections.

3) Barometric Measurements: In a realistic environment the height can be approximately calculated by measurements of air pressure p and temperature T as we will see in the following. To obtain realistic values for the pressure p and the temperature T for the artificial trajectories we also use random walk models for the reference values, where k denotes the sampling time:

$$p_0(k) = p_0(k-1) + \eta_{p_0}(k) \cdot \sqrt{\Delta t} \tag{3}$$

$$T_0(k) = T_0(k-1) + \eta_{T_0}(k) \cdot \sqrt{\Delta t} \tag{4}$$

with $\eta_{p_0}(k) \sim \mathcal{N}(0, \sigma_{p_0}^2)$ and $\eta_{T_0}(k) \sim \mathcal{N}(0, \sigma_{T_0}^2)$, where $\sigma_{p_0}^2$ and $\sigma_{T_0}^2$ are the variances of the normally distributed noise terms η_{p_0} and η_{T_0}. Note, that these equations only model the variations of pressure and temperature at reference height $h_0 = 0\,\text{m}$. The linear approximation between height (atmosphere) $h(k)$ and temperature is given by

$$T(k) = T_0(k) - a \cdot \Big(h(k) - h_0\Big), \tag{5}$$

where a is the positive lapse rate and $h(k)$ the height at time instance k. The following well known formula for the

isothermal atmosphere is now used to compute the pressure $p_h(k)$ for some height $h(k)$ [8]:

$$p_h(k) = p_0(k) \cdot \Big(1 - \frac{a \cdot \Delta h(k)}{T_0(k)}\Big)^{\frac{M \cdot g(\varphi(k))}{R \cdot a}}, \qquad (6)$$

where $\Delta h(k) = h(k) - h_0$ and where M is the molar mass, $g(\varphi)$ the gravity, depending on the current latitude φ of the user and R is the universal gas constant, respectively.

The artificial measurements are then computed by

$$\tilde{p}_h(k) = p_h(k) + w_{p_h}(k), \quad \tilde{T}(k) = T(k) + w_T(k), \qquad (7)$$

where $w_{p_h}(k)$ and $w_T(k)$ are normally distributed random variables with zero mean and variance $\sigma^2_{p_h}$ and σ^2_T, respectively: $w_{p_h}(k) \sim \mathcal{N}(0, \sigma^2_{p_h}), w_T(k) \sim \mathcal{N}(0, \sigma^2_T)$.

By using the formula for the isothermal atmosphere again, we get a measurement $z_h(k)$ for the barometric height by solving

$$\tilde{p}_h(k) = p_0(0) \cdot \Big(1 - \frac{a \cdot z_h(k)}{T_0(0)}\Big)^{\frac{M \cdot g(\varphi(k))}{R \cdot a}}. \qquad (8)$$

for $z_h(k)$. Note, that in contrast to eq. (6) we use the constant values $p_0(0)$ and $T_0(0)$ in eq. (8), since in a realistic environment, we would not have any knowledge about $p_0(k)$ and $T_0(k)$, respectively.

B. Field Data

We also used real-world measurements of an IMU, an altimeter and a GPS device to verify the experimental results based upon the artifically generated data. The Inertial Measurement Unit is a MotionNode device from GLI Interactive LLC. The GPS device (Navilock NL-402U) contains an ublox5 chipset, providing position and velocity estimates with a maximum rate of 4 Hz. The barometer is an OAK USB sensor device from Toradex, which provides pressure and temperature estimates at a rate of 10 Hz. The synchroneous recording of all information is handled by an external timer to guarantee that the synchronisation error is less than 1×10^{-9} s.

III. Loosely-Coupled Error State Space Kalman Filtering

A loosely-coupled error state space filter is often used in the context of IMU based navigation [2]. Fig. 2 shows the Kalman error filtering system in the upper part ①. It contains The IMU sensors, the GPS device, a block for the strapdown computation and the Kalman error filter. In this paper, we assume that the GPS sampling rate is 1 Hz while the sampling rate of the IMU is 50 Hz.

The strapdown block calculates the position of the IMU, its velocity, and the attitude, where the Bortz' differential equation

$$\dot{\boldsymbol{\zeta}} = \boldsymbol{\omega}^b_{nb} + \frac{1}{2}\boldsymbol{\zeta} \times \boldsymbol{\omega}^b_{nb} + \frac{1}{\boldsymbol{\zeta}^2}\Big(1 - \frac{\boldsymbol{\zeta}\sin(\boldsymbol{\zeta})}{2(1-\cos(\boldsymbol{\zeta}))}\Big)\boldsymbol{\zeta} \times (\boldsymbol{\zeta} \times \boldsymbol{\omega}^b_{nb}), \qquad (9)$$

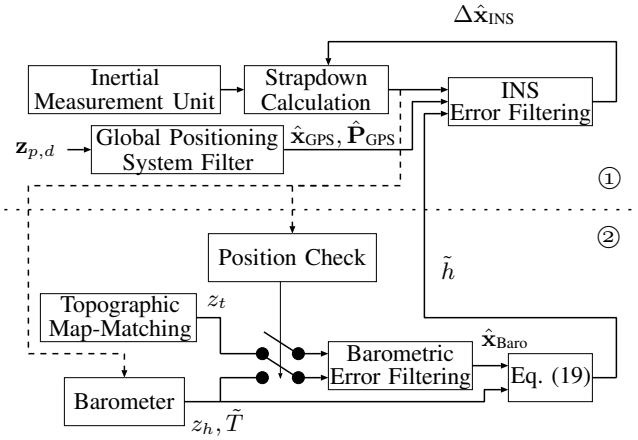

Fig. 2. Barometric error filtering with map-matching.

is used. Here, $\boldsymbol{\zeta}$ denotes the orientation vector and $\boldsymbol{\omega}^b_{nb}$ is the angular rotation vector of the body system with respect to the n-frame in coordinates of the navigation frame. Note, that the relation

$$\dot{\boldsymbol{\mu}} = \begin{bmatrix} 1 & \sin\phi\tan\theta & \cos\phi\tan\theta \\ 0 & \cos\phi & -\sin\phi \\ 0 & \sin\phi/\cos\theta & \cos\phi/\cos\theta \end{bmatrix} \boldsymbol{\omega}^b_{nb} \qquad (10)$$

holds. Further, eq. (11) describes the change of the velocity:

$$\dot{\mathbf{v}}^n_{eb} = \mathbf{C}^n_b \mathbf{a}^b_{ib} - (2\boldsymbol{\omega}^n_{ie} + \boldsymbol{\omega}^n_{en}) \times \mathbf{v}^n_{eb} + \mathbf{g}^n, \qquad (11)$$

where $\boldsymbol{\omega}^n_{ie}$ is the earth rotation rate vector depending on the current user position and $\boldsymbol{\omega}^n_{en}$ is the craft-rate in coordinates of the n-frame, which further depends on the user velocity vector $\mathbf{v}^n_{eb}$. We use $\mathbf{C}^n_b$ to denote the Direct Cosine Matrix, which transforms data from the body-frame into the n-frame. The gravity vector $\mathbf{g}^n$ has a single non-zero entry, which depends on the user latitude. For the update of the user position in the strapdown calculation we use the following equation with $v^n_{eb,n}$, $v^n_{eb,e}$ and $v^n_{eb,d}$ being the north, east and down components of the velocity vector, respectively:

$$\dot{\varphi} = \frac{v^n_{eb,n}}{R_n(\varphi) + h}, \quad \dot{\lambda} = \frac{v^n_{eb,e}}{(R_e(\varphi) + h)\cos(\varphi)}, \quad \dot{h} = -v^n_{eb,d}. \qquad (12)$$

Here, φ, λ and h denote latitude, longitude and height in direction away from the earth, respectively. The variables $R_n(\varphi)$ and $R_e(\varphi)$ are certain parameters of the WGS-84 earth model [1].

The Kalman filter state vector

$$\Delta\mathbf{x}_{\text{INS}} = [(\Delta\mathbf{p}^n)^T, (\Delta\mathbf{v}^n)^T, \Delta\boldsymbol{\Psi}^T, \Delta\mathbf{b}^T_a, \Delta\mathbf{b}^T_\omega]^T \qquad (13)$$

consists of the error of the position vector $\Delta\mathbf{p}^n$ in the n-frame, the error of the velocity vector $\Delta\mathbf{v}^n$, the error of the attitude vector $\Delta\boldsymbol{\Psi}$ and the vectors $\Delta\mathbf{b}_a$ and $\Delta\mathbf{b}_\omega$, which denote the biases of the accelerometer and the gyroscope, respectively. With the relation $\dot{\mathbf{C}}^n_b = \mathbf{C}^n_b \boldsymbol{\Omega}^b_{nb}$, where $\boldsymbol{\Omega}^b_{nb}$ is the skew symmetric matrix of $\boldsymbol{\omega}^b_{nb}$ and the differential equations (9) - (12) a system of differential equations can be

formed by Taylor series expansion. Then the state equations of the error state space Kalman filter are obtained by the subsequent discretization. The measurements for the loosely coupled filter are the (Kalman filtered) GPS outputs position and velocity, and the filtered barometer output.

The solution of the Taylor series expansion of the differential equations (9) - (12) around $\Delta\mathbf{x}_{\text{INS}}$ shows that there is an insufficient support of the yaw angle by the accelerometer measurements. Hence there is a need to use also measurements $\tilde{\mathbf{m}}^b$ of the terrestrial magnetic field, which depends on the attitude error through the following measurement equation:

$$\tilde{\mathbf{m}}^b(k) = (\hat{\mathbf{C}}_b^n)^T(k)\Big(\mathbf{m}^n + [\mathbf{m}^n\times]\Delta\boldsymbol{\Psi}(k)\Big) + \mathbf{w}_m(k). \quad (14)$$

The matrix $\hat{\mathbf{C}}_b^n$ denotes the corrected estimation of the DCM $\mathbf{C}_b^n$ and the constant vector $\mathbf{m}^n$ is assumed to be the true magnetic field with $\mathbf{m}^n = [19\,168.7\,\text{nT}, 418.0\,\text{nT}, 45\,077.9\,\text{nT}]^T$. These are realistic values for the magnetic field in Paderborn, Germany.

IV. Barometric Height Estimation with topographic Map-Matching

The height measurement system combined with map-matching is presented at the bottom of fig. 2 ②. A barometric height information is available with a rate of 10 Hz. When the distance between the current estimated position computed by the strapdown algorithm in combination with the GPS receiver and the barometer is less than $5\,\text{m}$ away from an entry of the topographic database (box denoted "Position Check"), the height read out of the topographic map is used in combination with the barometer reading for the error filtering. If not, only the barometer data are used. The heights in topographic maps are information with respect to the so-called ellipsoid, a specific earth model used for geodetic applications. In contrast a barometric device measures the height w.r.t. the so-called geoid. This difference has to be be accounted for in the comparison. Typical topographic maps can be found at [9]. Note, that there are often a couple of topographic lines crossing streets, where we assume that some of these crossing points are known and saved in the database.

We remember, that in a realistic scenario the variables $p_0(k)$ and $T_0(k)$ in eq. (6) are not known but constant values would be obtained. By substitution of $p_0(0)$ and $T_0(0)$ for $p_0(k)$ and $T_0(k)$ in eq. (6) and a Taylor series expansion around the triple $\big(h_0, T_0(0), p_0(0)\big)$, we obtain an approximate relation between the barometer measurements and the current height:

$$z_h(k) \approx \Big(1 + c_1(k)\Big)\cdot h(k) + c_2(k) + w_h(k), \quad (15)$$

with $w_h(k) \sim \mathcal{N}(0, \sigma_h^2)$. The scale factor $c_1(k)$ and the bias $c_2(k)$ depend on the errors in temperature and pressure as follows:

$$c_1(k) = \frac{\Delta T_0(k)}{T_0(0)}, \quad c_2(k) = \frac{R\cdot T_0(0)}{g(\varphi(k))}\cdot\frac{\Delta p_0(k)}{p_0(0)}, \quad (16)$$

where $\Delta T_0(k)$ and $\Delta p_0(k)$ denote the difference between the initial and current temperature and initial and current pressure at the reference height h_0, respectively: $\Delta T_0(k) = T_0(k) - T_0(0)$ and $\Delta p_0(k) = p_0(k) - p_0(0)$. We assume that the errors c_1 and c_2 can be modeled by random walk processes, where the variations in time are slow due to the relatively slow movement of the vehicle. With $\mathbf{x}_{\text{Baro}} = [c_1, c_2]^T$ we use

$$\mathbf{x}_{\text{Baro}}(k+1) = \mathbf{x}_{\text{Baro}}(k) + \boldsymbol{\eta}_{\text{Baro}}(k) \quad (17)$$

as state equation of the barometric error state Kalman filter, where the vector $\boldsymbol{\eta}_{\text{Baro}}$ consists of normally distributed random variables with zero mean and covariance matrix $\boldsymbol{\sigma}^2_{\text{Baro}}$. The measurement equation used for the topographic database entries is $z_t(k) = h(k) + w_t(k)$ with $w_t(k) \sim \mathcal{N}(0, \sigma_t^2)$.

In consideration of eq. (5) the input to this barometric error state Kalman filter is given by

$$\mathbf{z}(k) = \begin{pmatrix} z_h(k) - z_t(k) \\ \frac{\tilde{T}(k) + a\cdot z_t(k) - \hat{T}_0(0)}{\hat{T}_0(0)} \end{pmatrix} = \mathbf{H}_{\text{Baro}}(k)\cdot\mathbf{x}_{\text{Baro}}(k) + \mathbf{w}_{\text{Baro}}(k), \quad (18)$$

where the measurement matrix is given by $\mathbf{H}_{\text{Baro}}(k) = \begin{bmatrix} z_t(k) & 1 \\ 1 & 0 \end{bmatrix}$ and $\mathbf{w}_{\text{Baro}}(k) \sim \mathcal{N}(\mathbf{0}, \mathbf{R}_{\text{Baro}})$. The measurement covariance matrix is diagonal with $\mathbf{R}_{\text{Baro}} = \text{diag}\Big(\sigma_h^2 + (1+c_1)^2\cdot\sigma_t^2, \big(\frac{\sigma_T + a\cdot\sigma_t}{\hat{T}_0(0)}\big)^2\Big)$,where $\hat{T}_0(0)$ denotes the initial assumption for $T_0(0)$. Note, that in eq. (18) $z_t(k)$ on the right side is assumed to be deterministic.

In the last step the barometric errors are used for the error correction of the barometric height estimates. This is done by rearranging eq. (15):

$$\tilde{h}(k) = \frac{z_h(k) - \hat{c}_2(k)}{1 + \hat{c}_1(k)}, \quad (19)$$

where $\hat{c}_1, \hat{c}_2$ denote the estimates of the barometric error filter. They are set constant to the last estimates, if there is no topographic database entry available for updating.

V. Experimental Results

In this section we present experimental results concerning the quality of the proposed algorihm. The horizontal root mean square (RMS) error of the simulated GPS positions after filtering is about $4\,\text{m}$, while the vertical error is about $10\,\text{m}$. In realistic scenarios the accuracy of the GPS estimates mainly depends on the DOP (Dilution of precision) value, which specifies the effect of GPS satellite constellation on the positioning error. Further, the error of the horizontal velocity components is $0.5\,\frac{\text{m}}{\text{s}}$ and for the vertical component $1.5\,\frac{\text{m}}{\text{s}}$, respectively. The standard deviation of the accelerometer biases is $\sigma_{b_a} = 3.3\,\frac{\text{m/s}^2}{\sqrt{\text{s}}}$ for every entry in the vector $\boldsymbol{\eta}_a$, while the standard deviation of the equivalent inherent noise term is $\sigma_a = 35\times10^{-4}\,\frac{\text{m/s}^2}{\sqrt{\text{s}}}$ according to the realistic data given in [7] [1]. The corresponding gyroscope values are for the biases $\sigma_{b_\omega} = 0.0167\,\frac{\text{deg/s}}{\sqrt{\text{s}}}$ and for the inherent noise $\sigma_\omega = 10.61\times10^{-2}\,\frac{\text{deg}}{\sqrt{\text{s}}}$. The standard deviation of

[1] Note, that it holds: $1\,\frac{\text{m/s}^2}{\sqrt{\text{s}}} = 101.97\,\frac{\text{mg}}{\sqrt{\text{Hz}}} = 60\,\frac{\text{m/s}}{\sqrt{\text{h}}}$

the inherent noise of the magnetometer is $12.94\,\frac{\mathrm{nT}}{\sqrt{\mathrm{s}}}$ for each component. The standard deviation σ_t is set to zero, while $\sigma_h \propto \sigma_{p_h}$.

The initial temperature is assumed to be $T_0(0) = 288.15\,\mathrm{K}$ while the initial pressure is $p_0(0) = 1013.15\,\mathrm{hPa}$. The inherent measurement noise of the temperature is assumed to have a standard deviation of $\sigma_T = 0.2\,\mathrm{K}$. The corresponding pressure value is $\sigma_{p_h} = 10\,\mathrm{Pa}$. The standard deviations of pressure and temperature at reference height h_0 are $\sigma_{p_0} = 0.4\,\frac{\mathrm{Pa}}{\sqrt{\mathrm{s}}}$ and $\sigma_{T_0} = 0.004\,\frac{\mathrm{K}}{\sqrt{\mathrm{s}}}$.

First, we want to present results for artificially generated data. The duration of the simulated drive is $3.500\,\mathrm{s}$. We assume, that a reference height of the topographic map database, to be used for error estimation in the barometric height filter, is available every $100\,\mathrm{s}$, where the database contains 10.000 entries. This could be a realistic database size for a considered map section of about $40\,\mathrm{km} \times 40\,\mathrm{km}$.

A. Localization performance

Fig. 3 displays the absolute height estimation error $|h(k) - \hat{h}(k)|$ over time for the individual approaches for a trajectory of duration $200\,\mathrm{s}$. The height estimates provided by GPS

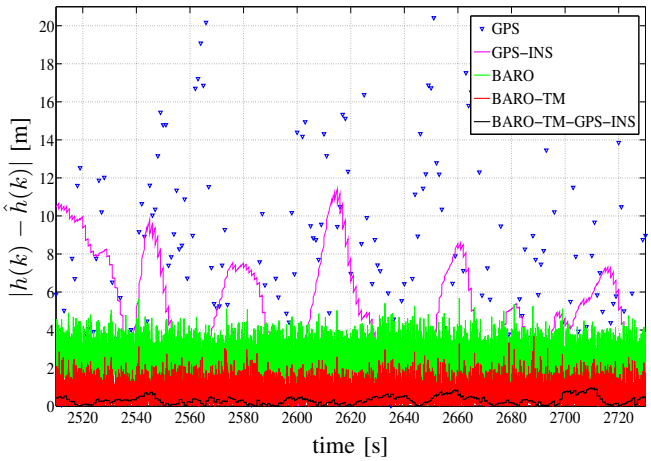

Fig. 3. Absolute error of height estimates.

(denoted by GPS) exhibit the largest errors compared to the other approaches. The INS based estimate which is only aided by GPS data (GPS-INS) is also illustrated for reference.

The absolute error of the unfiltered barometric measurements (denoted by BARO) achieves an average error of about $5\,\mathrm{m}$. Higher precision is obtained by the corrected barometric estimates $\tilde{h}$ (BARO-TM) aided by topographic map-matching is of higher accuracy. Due to the barometric error filter the barometric height become more reliable even if there is no reference height from a topographic map is available. Further, we see that the combined approach (BARO-TM-GPS-INS) outperforms the other algorithms: The estimation error is less than $1\,\mathrm{m}$ in almost all cases.

In fig. 4 and fig. 5 the cumulative density functions of the position error and the velocity error of the different approaches are illustrated. Here, BARO-TM-GPS-INS denotes again the combined estimator with topographic map-matching, GPS the solely filtered GPS measurements and GPS-INS is the filter stage, using GPS based height estimates instead of barometer based height estimates for the correction of the attitude of the IMU. It can be seen that using a barometer in combination

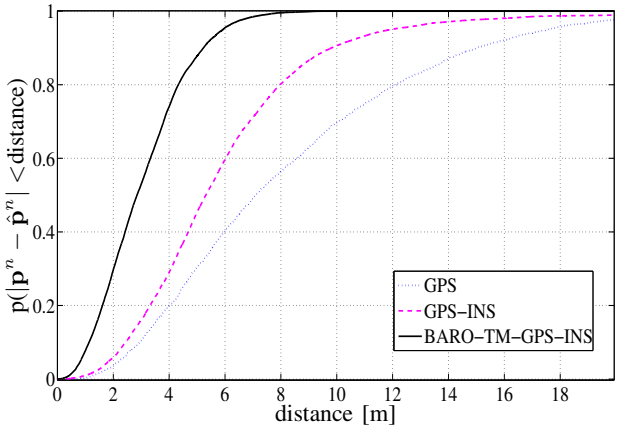

Fig. 4. Cumulative density functions (CDF) of positioning error.

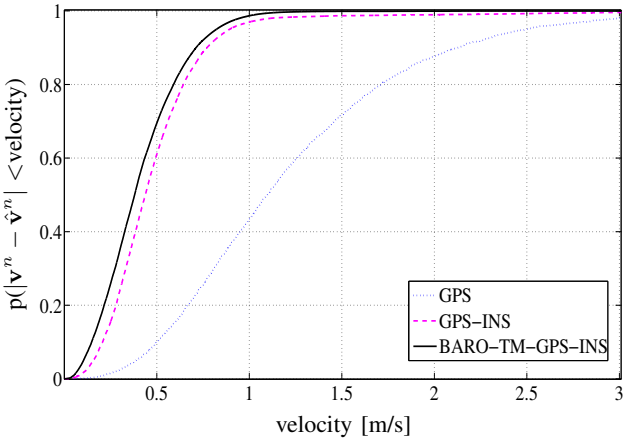

Fig. 5. Cumulative density functions (CDF) of velocity error.

with map matching improves the performance of a GPS aided IMU. Note, that the gain in position accuracy is not only due to the improved vertical component. The usage of a barometer also improves the horizontal position estimates of the GPS-INS filter. This can be explained by the fact that there is a dependence of the horizontal components of the attitude error $\Delta\boldsymbol{\Psi}$ in the vector $\Delta\mathbf{x}_{INS}$ on the height measurement $\tilde{h}$, if the position of the GPS antenna in the body system of the IMU is known.

B. Barometric Error Filter

In this section we describe some results concerning the performance of the barometric error Kalman filter. This filter is meant to estimate the parameters c_1 and c_2 of the approximate barometer equation (15). The figs. 6 and 7 show trajectories of

the true values of the parameters c_1 and c_2 and their estimates. At the beginning of the simulation the estimates, notably

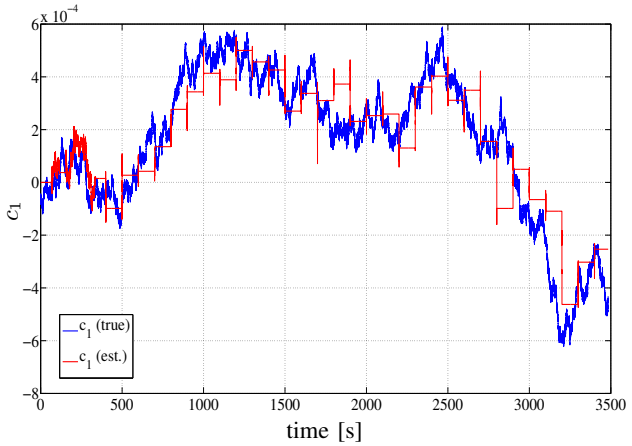

Fig. 6. Barometric scale error c_1 (est.: estimated values).

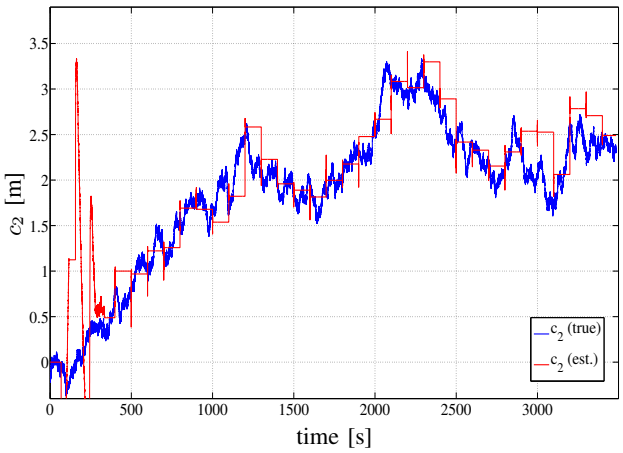

Fig. 7. Barometric bias error c_2 (est.: estimated values).

of c_2, are inaccurate due to inappropriate initialization and the unavailability of reference height values. From $t = 400\,\mathrm{s}$ on the estimates are close to the true values. Note, that the parameter estimates are only updated when a topographic map value is available. As this occurs only every $t = 100\,\mathrm{s}$ the computational effort is small. Remember that the factor c_1 can be seen as a scale error mainly caused by errors in the temperature measurement and c_2 is the bias due to errors in pressure measurements.

C. Complexity

Although the proposed algorithm seems to be computationally demanding, the effort compared to other methods can be justified by its superior performance. The main difference between our solution and a typical loosely coupled filter is the second Kalman filter for estimating the parameters of the barometer. However, the dimension of the state vector is only (2×1). Thus, the computational effort is insignificant compared to the effort spent on the loosely coupled filter, whose state vector is of dimension (15×1).

In tab. I we present the mean elapsed times of the different blocks of our approach for different artifical trajectories and a computed data set of duration of $1\,\mathrm{s}$, because this is the usual sampling time of a GPS receiver. The simulations had been carried out using Matlab R2008b on a $2.33\,\mathrm{GHz}$ Quad-Core Xeon Processor with $4\,\mathrm{GB}$ RAM. The figures in the table confirm that the effort spent on the barometric filter is negligible.

Strapdown	Barometric filter	Database search	Loosely coupled filter
$18.2 \times 10^{-3}\,\mathrm{s}$	$0.91 \times 10^{-3}\,\mathrm{s}$	$8.7 \times 10^{-3}\,\mathrm{s}$	$28.8 \times 10^{-3}\,\mathrm{s}$

TABLE I
RUNTIMES OF STAGES.

D. Field measurements

We want to complete the section with some experimental results using field data gathered during a test drive of about $50\,\mathrm{m}$ which included sections in an urban environment and sections in a rural environment. The velocity varied between $0\,\frac{\mathrm{km}}{\mathrm{h}}$ (e.g. due to stops at traffic lights) and $120\,\frac{\mathrm{km}}{\mathrm{h}}$ (e.g. on a highway). Fig. 8 shows a map of a part of the route. It also depicts the location of the waypoints. For every waypoint we assume that a topographic height is available.

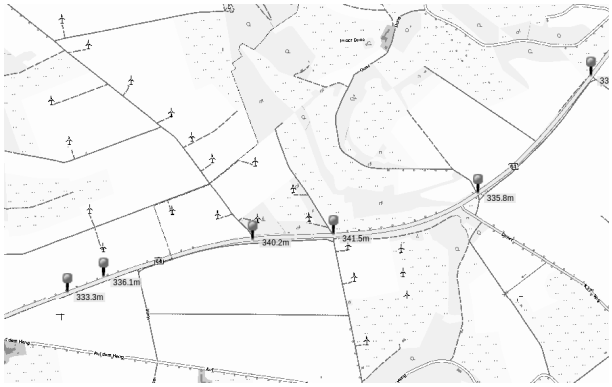

Fig. 8. Route section with markers, where a topographic height is known.

In fig. 9 some results concerning the height accuracy are presented. It seems that the unfiltered barometric measurements (BARO) are affected by a constant bias. The barometric Kalman filter seems to track the bias c_2 well, as the corrected values (BARO-TM) no longer exhibit a bias. The differences between the height estimates of the combined filter (BARO-TM-GPS-INS) and the GPS based height estimates seem to be up to $25\,\mathrm{m}$, while the corrected barometric estimates BARO-TM are close to the combined estimator using reference points. Further in our examinations seem to be only little variations between the estimated heights at the output of the strapdown block and the reference heights, considering sections, where no

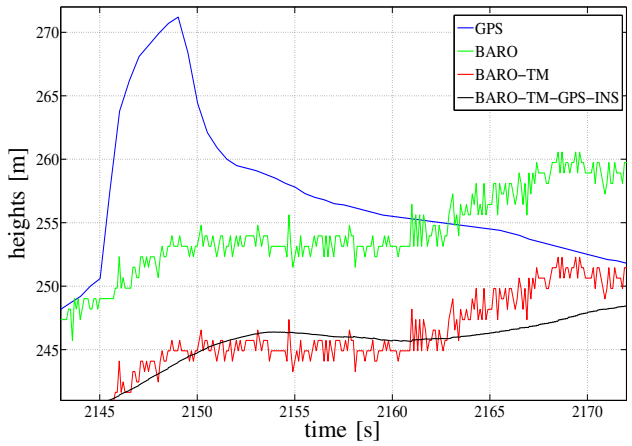

Fig. 9. Measured and estimated heights along a part of the route during field trial.

reference height could be used for the update of the barometric Kalman filter.

Fig. 10 shows the true theoretical scale factor c_1 compared to the filtered estimates. Due to the lack of a sufficient amount of reliable reference measurements of the pressure, we considered here only the temperature in detail. It is shown

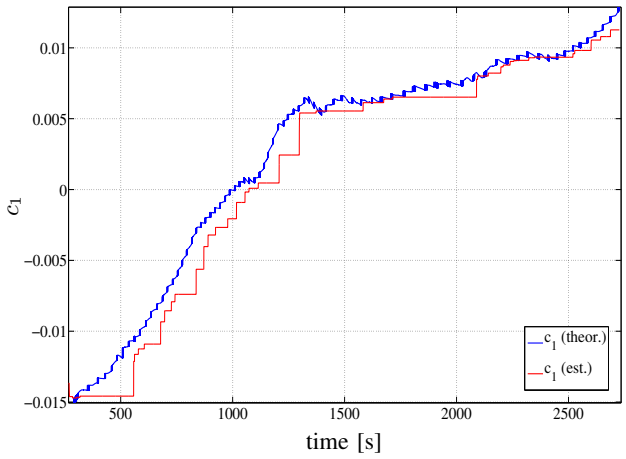

Fig. 10. Theoretical and estimated scale factor c_1.

that the estimated values of the scale factor c_1 stay close to the true ones, which were given by the mean of the measured temperatures of different temperature devices and the assumptions that $T_0(0) = 281.06\,\mathrm{K}$ and $p_0(0) = 1018.23\,\mathrm{hPa}$, which were measured by a barometrical reference station.

The last figure 11 illustrates the reliability of the proposed algorithm when GPS dropouts occur. When we consider the section, where a dropout is present for a duration of about 25 s (green dotted line marks the GPS availability), we recognize that the estimated trajectory (red line) is close to the real one (blue line). Note, that the direction of motion changes very fast at a certain point in the middle of the figure, which is however detected by the system very well. Certainly, similar results are also feasible, when the IMU is aided by a GPS

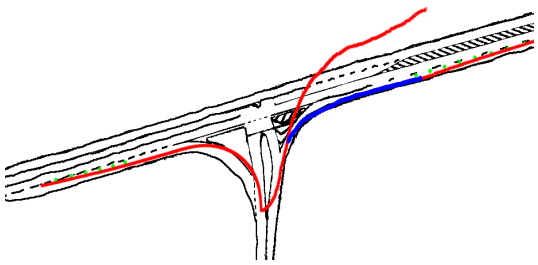

Fig. 11. Simulated GPS dropout for real trajectory.

device solely. But, as mentioned before, the result does not only rely on the IMU alone. The improvement arises from the combination of both, the IMU and the barometer since there exist correlations between the height estimates and the attitude errors in all axes of the IMU, which are filtered in the GPS-INS filter. If employing only the height component of a GPS device for aiding the IMU, the attitude would be corrected much poorer due to the low quality of the height estimates of the GPS Kalman filter.

VI. Conclusions

In this paper, a sensor fusion algorithm based on an IMU, a GPS device and a barometer is proposed for a robust vehicle localization. The error of the barometric device is kept small by using reference heights from a topographical map and an error state Kalman filter for compensating unwanted variations. The proposed algorithm outperforms a common method of height estimation which is based on the vertical position information of a GPS device together with an IMU device. It is shown that the additional usage of a barometer instead of a GPS device alone results in better attitude corrections due to correlations between the barometric height and the error vector of the attitude of the IMU depending on the current DCM estimate and the GPS antenna position. In further work we will explore the potential of our approach for indoor localization.

References

[1] J. Wendel, *Integrierte Navigationssysteme*, Oldenbourg, 2007.
[2] M. Titterton, *Estimation with Applications to Tracking and Navigation*, John Wiley & Sons, Inc., 2001.
[3] Y. Bar-Shalom, X. R. Li, and T. Kirubarajan, *Estimation with Applications to Tracking and Navigation*, John Wiley & Sons, Inc., 2001.
[4] J. Farrell and M. Barth, *The Global Positioning System and Inertial Navigation*, McGraw-Hill, 1998.
[5] C. Jekeli, *Inertial Navigation Systems with Geodetic Applications*, de Gryter, 2001.
[6] M. Bevermeier, S. Peschke, and R. Haeb-Umbach, *Robust Vehicle Localization based on Multi-Level Sensor Fusion and Online Parameter Estimation*, *WPNC'09*, 2009.
[7] GLI Interactive LLC, *MotionNode specifications*, http://www.motionnode.com/products.html, 2009.
[8] National oceanic and amospheric administration, *U.S. Standard atmosphere*, 1976.
[9] East view cartographic, *Topographic Maps*, http://www.cartographic.com/, 2010.